Journal of Alloys and Compounds 481 (2009) 75–80

Contents lists available at ScienceDirect

Journal of Alloys and Compounds

journal homepage: www.elsevier.com/locate/jallcom

Electronic structure and magnetic properties of transition metal diborides

G.E. Grechnev[a], A.V. Fedorchenko[a], A.V. Logosha[a], A.S. Panfilov[a,*], I.V. Svechkarev[a], V.B. Filippov[b], A.B. Lyashchenko[b], A.V. Evdokimova[b]

[a] B. Verkin Institute for Low Temperature Physics and Engineering, 47 Lenin Ave., 61103 Kharkov, Ukraine
[b] I. Frantsevich Institute for Problems of Material Science, 3 Krzhyzhanovsky Street, 03680 Kiev, Ukraine

ARTICLE INFO

Article history:
Received 28 January 2009
Received in revised form 19 March 2009
Accepted 21 March 2009
Available online 31 March 2009

PACS:
71.20.−b
72.80.Ga
75.10.Lp
75.30.Gw

Keywords:
Diborides
Electronic structure
Magnetic susceptibility
Magnetic anisotropy

ABSTRACT

The temperature dependencies of the magnetic susceptibility χ and its anisotropy $\Delta\chi = \chi_{\parallel} - \chi_{\perp}$ were measured for the hexagonal single crystalline TB_2 compounds (T = Sc, Ti, Zr, Hf, V and Cr) in the temperature range 4.2–300 K. It was found that $\Delta\chi$ varies strongly and nonmonotonously with the filling of the hybridized *d*-band, being almost temperature independent and the largest for the diborides of group 4 metals. *Ab initio* calculations of the electronic structure and susceptibility of the diborides provide evidence that magnetic anisotropy originates from competing Van Vleck paramagnetism and the orbital diamagnetism of conduction electrons.

1. Introduction

Transition metal (T) diborides TB_2 are of great scientific and technological interest due to their unique physical and chemical properties such as high melting point, hardness, thermal conductivity, and chemical inertness [1]. The most known TB_2compounds are diborides of transition metals of groups 3–6 (Sc, Ti, Zr, Hf, V, Nb, etc.) which have the layered hexagonal *C*32 structure of AlB_2 type. These compounds retain the *C*32 crystal structure in a wide range of conduction band occupation numbers in respective 3*d*-, 4*d*- and 5*d*-series, providing a variety of structural, electronic and magnetic properties [1–7].

The discovery of superconductivity in MgB_2at $T = 39$ K has initiated detailed studies of superconducting and other physical properties of AlB_2-type borides, and there are controversial and contradictory reports on the superconductivity and value of T_c for TB_2 (see e.g. [5] and references therein). Also, there is only scarce and incomplete information on magnetic properties of diborides [1–3]. Despite a great number of experimental studies in the past years, the available data on superconducting, magnetic and elastic properties of $TB_2$are still limited and ambiguous. Also these data were mostly obtained for the polycrystalline samples of different quality and origin. The recent technological progress in growing the single crystal samples has made possible more detailed and extended experimental investigations of the physical properties of diborides, including studies of the Fermi surface features and manifestations of the lattice anisotropy by using the de Haas–van Alphen effect [6].

In this paper we present results of experimental and theoretical investigations of magnetic properties of the single crystalline diborides TB_2in relation to their electronic structure. The main objective of this work is to study the magnetic susceptibility and its anisotropy in the representative series of the *C*32 diborides. These diborides appear to be an appropriate set of the isostructural compounds, allowing to analyse variations of the magnetic properties with substantial changes in lattice parameters and the filling of strongly hybridized *p*–*d* states.

The detailed experimental studies of magnetic susceptibility for TB_2 compounds are supplemented by electronic structure calculations within LSDA approximation of the density-functional theory by using a full-potential LMTO method. Within the unified *ab initio* approach, the electronic structure, magnetic and elastic properties of ScB_2, TiB_2, VB_2, CrB_2, ZrB_2, and HfB_2 were evaluated and compared with experimental data.

* Corresponding author. Fax: +380 573 403 370.
E-mail address: panfilov@ilt.kharkov.ua (A.S. Panfilov).

0925-8388/$ – see front matter © 2009 Elsevier B.V. All rights reserved.
doi:10.1016/j.jallcom.2009.03.123

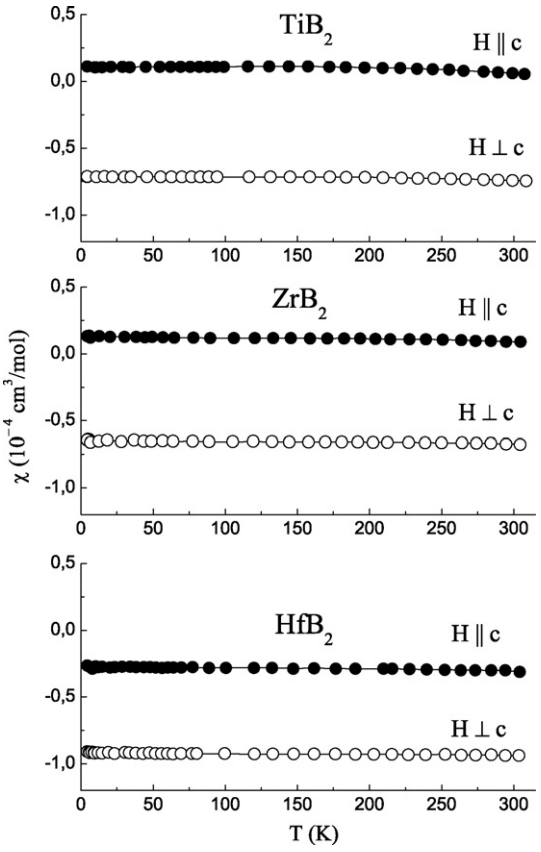

Fig. 1. Temperature dependence of the magnetic susceptibility for the diborides of group 4 metals.

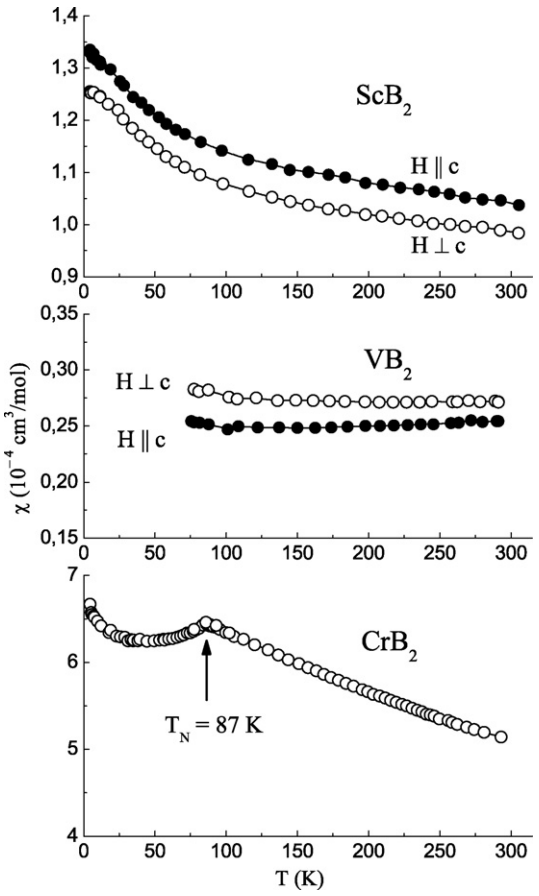

Fig. 2. Temperature dependence of the magnetic susceptibility for ScB_2, VB_2 and CrB_2 compounds.

2. Experimental details and results

The diborides single crystals were obtained by high-frequency crucibleless zone melting of the initial diborides powders prepared by reduction of the oxides of the corresponding metals of 99.95% purity with amorphous boron of 99.9% purity (for details see Refs. [6,8]). The de Haas–van Alphen effect has been recently reported [6] for the same set of samples that supports their high quality. The measurements of the magnetic susceptibility and its anisotropy were carried out by a Faraday method in the temperature range 4.2–300 K and in magnetic field around $H \simeq 1$ T.

The magnetic susceptibility of diborides versus temperature $\chi(T)$ was measured for the magnetic field applied both along and perpendicular to the six-fold c-axis of the hexagonal structure, $\chi_\parallel$ and $\chi_\perp$, respectively. As seen in Figs. 1 and 2, in most cases the $\chi(T)$ dependence is rather weak, except for ScB_2 and CrB_2, and the magnetic anisotropy $\Delta\chi = \chi_\parallel - \chi_\perp$ appears to be nearly temperature independent. Also, in the series of TB_2 $\Delta\chi$ reveals a strong and nonmonotonous dependence on the conduction band filling, and the largest anisotropy is found for the diborides of group 4 metals.

CrB_2 is the first magnetic compound in the series, which orders antiferromagnetically (AFM) with the Néel temperature $T_N = 85$–88 K [2,9,10]. According to the neutron-diffraction measurements [9], CrB_2 possesses a helical magnetic structure of cycloidal type, which magnetic moment (of about 0.6 μ_B per Cr atom at $T = 0$) turns in the a–c plane. As it follows from the available data on magnetic properties of the single crystalline CrB_2 sample [10], in the paramagnetic (PM) phase the susceptibility of CrB_2 is an order of magnitude higher than that of other diborides, and there is no noticeable anisotropy of χ in this compound. Our data in Fig. 2 corresponds to a polycrystalline sample of CrB_2, and appears to be in agreement with the results of Ref. [10]. The distinctive feature of the observed $\chi(T)$ is a sharp cusp at $T_N \simeq 87$ K, where the AFM–PM transition takes place.

The room temperature values of the magnetic susceptibility and its anisotropy for the studied diborides are summarized in Table 1 together with the available experimental data. As seen from the table, for some systems, especially the diborides of group 4 metals, there is a noticeable discrepancy between our results and the literature data obtained for polycrystalline samples. This suggests that magnetic susceptibility of the diborides is strongly dependent on a sample quality and its stoichiometry.

3. Computational details and results

3.1. Band structure calculations

The investigated diborides possess the hexagonal $C32$ crystal structure with c/a ratio close to unity [1]. This crystal lattice is composed of transition metal layers alternating with graphite-like boron layers stacked perpendicularly to the [0 0 1]axis. *Ab initio* calculations of the electronic structure of diborides were carried out by employing a modified FP-LMTO method [14,15]. The exchange-correlation potential was treated in the LDA [16] and GGA [17] approximations of the density functional theory. In the present calculations for TB_2 the FP-LMTO basis set included the 2s, 2p, and 3d orbitals of boron, as well as the np, $(n+1)s$, $(n+1)p$, and nd orbitals of T within a single, fully hybridizing energy panel, where n is the principal quantum number for d valence states of the transition metal.

The integration over the Brillouin zone was performed using the tetrahedron method [18]. The results reported here were obtained by using up to 4000 k-points in the irreducible wedge of the Brillouin zone for the field-induced spin-polarized calculations described below. The corresponding calculated total energies were well converged ($\sim 10^{-6}$ Ry) with respect to all parameters involved, such as k-space sampling and basis set truncation.

The band structure calculations were performed for a number of lattice parameters close to the experimental ones, and the c/a ratio was fixed at its experimental value for each TB_2 compound. The equilibrium lattice spacings and corresponding theoretical bulk moduli B_{LDA} were determined from calculated (within LDA) volume dependencies of the total energy $E(V)$ by employing the well known

Table 1
Magnetic susceptibility of TB_2 at $T = 293$ K.

TB_2	$\chi_\parallel$ ($\times10^{-4}$ cm^3/mol)	$\chi_\perp$ ($\times10^{-4}$ cm^3/mol)	$\chi_\parallel - \chi_\perp$ ($\times10^{-4}$ cm^3/mol)	$\bar{\chi} = (\chi_\parallel + 2\chi_\perp)/3$ ($\times10^{-4}$ cm^3/mol)	
ScB_2	1.045	0.989	0.056	1.008	~0.8 [a]
TiB_2 [b]	0.066	−0.740	0.806	−0.471	−0.40 [c]; 0.31 [d]
ZrB_2	0.094	−0.671	0.765	−0.416	−0.68 [d]
HfB_2	−0.303	−0.936	0.633	−0.725	−0.04 [d]
VB_2	0.255	0.271	−0.016	0.265	0.21 [c]; 0.34 [d]
CrB_2	–	–	~ 0 [e]	5.14	5.4 [e]; 3.9 [d]
NbB_2	–	–	–	–	0.08 [d]
TaB_2	–	–	–	–	−0.65 [d]

[a] Ref. [11].
[b] The sample was kindly presented by F.A. Sidorenko.
[c] Ref. [12].
[d] Ref. [13].
[e] Ref. [10].

Table 2
Experimental lattice parameters (from Ref. [1]), calculated bulk moduli B and contributions to magnetic susceptibility of diborides (see text for details).

TB_2	a (Å)	c (Å)	B (GPa)	χ_{ston} ($\times10^{-4}$ cm^3/mol)	$\bar{\chi}_{spin}$ ($\times10^{-4}$ cm^3/mol)	$\bar{\chi}_{orb}$ ($\times10^{-4}$ cm^3/mol)	$\Delta\chi_{orb}$ ($\times10^{-4}$ cm^3/mol)	χ_{dia} ($\times10^{-4}$ cm^3/mol)	χ_{sum} [a] ($\times10^{-4}$ cm^3/mol)
ScB_2	3.148	3.516	240	0.40	0.57	0.39	0.043	−0.10	0.86
TiB_2	3.028	3.228	290	0.10	0.15	0.99	0.131	−0.12	1.02
VB_2	2.998	3.057	270	0.68	0.90	0.83	0.080	−0.11	1.62
CrB_2	2.969	3.066	230	4.0	7.03	0.60	0.010	−0.10	7.53
YB_2	3.298	3.843	230	0.39	0.43	0.23	0.025	−0.25	0.41
ZrB_2	3.165	3.547	280	0.08	0.09	0.50	0.053	−0.23	0.36
NbB_2	3.115	3.264	260	0.38	0.40	0.56	0.068	−0.22	0.74
MoB_2	3.040	3.120	250	0.58	0.62	0.55	0.008	−0.20	0.97
HfB_2	3.140	3.470	310	0.07	0.09	0.41	0.032	−0.36	0.14
TaB_2	3.097	3.225	290	0.35	0.37	0.47	0.055	−0.35	0.49

[a] $\chi_{sum} = \bar{\chi}_{spin} + \bar{\chi}_{orb} + \chi_{dia}$.

Murnaghan equation [14]. This equation is based on the assumption that the pressure derivative B' of the bulk modulus B is constant. By using the values of B', evaluated from the Murnaghan equation, we have estimated bulk moduli B, corresponding to the *experimental* lattice parameters, and these estimations are given in Table 2.

According to our previous calculations [15,19], such corrections for B_{LDA} provided the theoretical estimations of B close to experimental values of the bulk moduli. The obtained high values of bulk moduli of diborides (Table 2) are in a qualitative agreement with the theoretical B of Ref. [7], calculated within DFT-GGA approximation. Though there are scarce and contradictory experimental data on elastic properties of diborides (see Refs. [7,1] and references therein), the results of present calculations, as well as ones of Ref. [7], allow to reveal the trends of bulk moduli behavior among diborides and to supplement deficient experimental data. This is of particular importance in connection with the recently found very high bulk moduli in the ultraincompressible diborides RuB_2, OsB_2 and ReB_2 [20], having somewhat different crystal structure [1]. The present results also indicate, that previously reported in Ref. [4] theoretical bulk moduli of the hexagonal $C32$ diborides were substantially underestimated, presumably due to the employed atomic sphere approximation for the total energy calculations.

As seen in Figs. 3 and 4, the calculated densities of electronic states (DOS) $N(E)$ of the diborides are similar, but vary in details and positions of the Fermi level E_F. The vertical lines in Figs. 3 and 4 indicate the conduction band filling for the corresponding 3d- and 4d-diborides. According to the calculations, the partial DOSs in Figs. 3 and 4 exhibit a strong hybridization of d-states of transition metal with p-states of boron. Also, in addition to the p–d hybridization, the filling of conduction band is expected to be substantially responsible for properties of transition metal diborides.

For the diborides of metals from group 4 (TiB_2, ZrB_2, HfB_2) and 5 (VB_2, NbB_2, TaB_2) the bonding states are filled, whereas antibonding states are almost unoccupied. This can explain hardness and high chemical stability of these borides. Within the series ScB_2–MnB_2, and also YB_2–MoB_2, the Fermi level passes through a deep minimum in DOS $N(E)$, related to the pseudo-gap in electronic spectrum, and falls into the area of antibonding states and large values of $N(E_F)$. Consequently, this leads to instability of the $C32$ phase of diborides from the middle of the transition metals row.

3.2. Calculated magnetic properties

The FP-LMTO calculations of the field-induced spin and orbital (Van Vleck) magnetic moments were carried out for the diborides

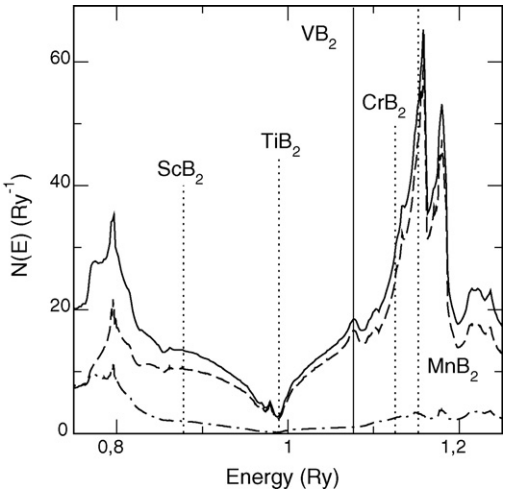

Fig. 3. Density of states for VB_2. The total DOS and partial contributions of vanadium d-states and boron p-states are indicated by solid line, dashed line, and dashed-dotted line, respectively. The vertical lines mark the conduction band filling for the corresponding 3d-diborides.

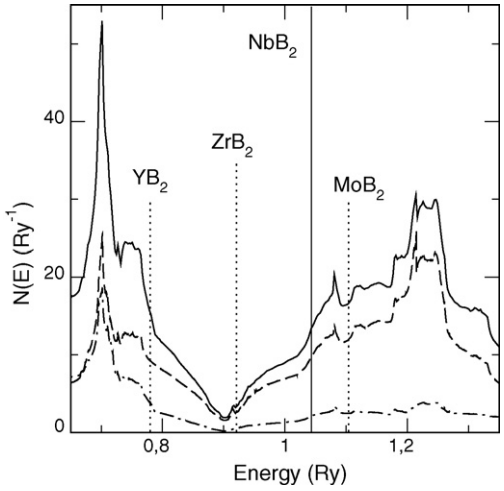

Fig. 4. Density of states for NbB_2. The total DOS and partial contributions of niobium *d*-states and boron *p*-states are indicated by solid line, dashed line, and dashed-dotted line, respectively. The vertical lines mark the conduction band filling for the corresponding 4*d*-diborides.

in the external field H of 10 T. The effect of the external magnetic field was taken into account self-consistently, within LSDA in line with the method described in Refs. [15,19], by means of the Zeeman operator:

$$\hat{H}_Z = \mathbf{H} \cdot (2\hat{\mathbf{s}} + \hat{\mathbf{l}}), \tag{1}$$

which was incorporated in the FP-LMTO Hamiltonian. Here $\hat{\mathbf{s}}$ is the spin operator and $\hat{\mathbf{l}}$ the orbital angular momentum operator. When the field-induced spin and orbital magnetic moments are calculated, the corresponding volume magnetization can be evaluated, and the ratio between the magnetization and the field strength provides the related contributions to susceptibility, $\chi_{\rm spin}$ and $\chi_{\rm orb}$.

For the hexagonal $C32$ crystal structure, the components of these contributions, $\chi_{i\parallel}$ and $\chi_{i\perp}$, are derived from the magnetic moments obtained in an external field, applied parallel and perpendicular to the *c*-axis, respectively. The averaged values of the calculated $\chi_{\rm spin}$ and $\chi_{\rm orb}$ components $\bar{\chi}_i = (\chi_{i\parallel} + 2\chi_{i\perp})/3$ and the evaluated anisotropy of the orbital contribution $\Delta\chi_{\rm orb} = \chi_{{\rm orb}\parallel} - \chi_{{\rm orb}\perp}$ are listed in Table 2. The employed number of 4000 k-points provides relative precision better than 10% for the calculated $\Delta\chi$, or about $10^{-5}\mu_B$ for corresponding field-induced moments, using the external field of 10 T.

For comparison, the Pauli spin contribution to the magnetic susceptibility was calculated within the Stoner model:

$$\chi_{\rm ston} = S\chi_{\rm P} \equiv \mu_{\rm B}^2 N(E_{\rm F})[1 - IN(E_{\rm F})]^{-1}, \tag{2}$$

where $\chi_{\rm P} = \mu_{\rm B}^2 N(E_{\rm F})$, S is the Stoner enhancement factor, and $\mu_{\rm B}$ the Bohr magneton. The Stoner integral I, describing the exchange-correlation interaction of the conduction electrons can be expressed in terms of the calculated parameters of the electronic structure (see Ref. [21] and references therein):

$$I = \frac{1}{N(E_{\rm F})^2} \sum_{qll'} N_{ql}(E_F) J_{qll'} N_{ql'}(E_F). \tag{3}$$

Here $N(E_{\rm F})$ is the total density of electronic states at the Fermi level $E_{\rm F}$, $N_{ql}(E_{\rm F})$ is the partial density of states for atom q in the unit cell, $J_{qll'}$ are the local exchange integrals:

$$J_{ll'} = \int g(\rho(r))\phi_l(r)^2 \phi_{l'}(r)^2 \, {\rm d}r, \tag{4}$$

where $\phi_l(r)$ are the partial wave functions, and $g(\rho(r))$ is a function of the charge density [16]. The values of the calculated enhanced Pauli susceptibility $\chi_{\rm ston}$ are also presented in Table 2.

4. Discussion

The calculation of the magnetic susceptibility of metallic systems is a rather difficult problem (see [15,22] and references therein). The total susceptibility in the absence of spontaneous magnetic moment can be expressed as the sum:

$$\chi_{\rm tot} = \chi_{\rm spin} + \chi_{\rm orb} + \chi_{\rm dia} + \chi_{\rm L}, \tag{5}$$

where these terms correspond to the Pauli spin susceptibility, a generalization of the Van Vleck orbital paramagnetism, the Langevin diamagnetism of closed shells, and generalization of Landau conduction electrons diamagnetism, respectively. The Langevin contributions $\chi_{\rm dia}$ were estimated based on results of Refs. [22–24] and appeared to be between free-atom and free-ionic diamagnetic susceptibilities (see Table 2). Obviously, these $\chi_{\rm dia}$ terms do not reveal any anisotropy.

In order to analyse the experimental data on χ and $\Delta\chi$ we use the calculated contributions to χ in Table 2. As can be seen from the table, in the non-magnetic transition metal diborides the orbital Van Vleck term $\chi_{\rm orb}$ provides substantial contribution to the total paramagnetic susceptibility. In some diborides $\chi_{\rm orb}$ even overcomes $\chi_{\rm spin}$, particularly this shows up in the diborides of group 4 metals (TiB_2, ZrB_2, HfB_2). Also, it can be seen in Table 2 that the Stoner model provides smaller values of the spin susceptibility $\chi_{\rm ston}$, comparatively to the field-induced calculated $\chi_{\rm spin}$. This is in agreement with the recent observation [19], that for the paramagnetic metallic systems the Stoner approach underestimates spin susceptibility, whereas the LSDA field-induced calculations take into account non-uniform induced magnetization density in the unit cell and provide more accurate values of $\chi_{\rm spin}$.

To calculate the Landau diamagnetic contribution $\chi_{\rm L}$ is a considerably more difficult problem (see [22,25–27] and Refs. therein). The free-electron Landau limit is often used for estimations, giving a $\chi_{\rm L}^0$ that equals $-(1/3)$ of the Pauli spin susceptibility, though for many systems this crude approximation was found not to provide even the correct order of magnitude of the diamagnetic susceptibility [25,27–29].

According to the experimental data in Table 1 and Figs. 1 and 2, the observed anisotropy of susceptibility appears to be the largest and almost temperature independent for the diborides of group 4 metals. As can be seen in Table 2, the calculated anisotropy of the Van Vleck paramagnetic contribution $\chi_{\rm orb}$ ranges only from 5 to 15% of the experimental $\Delta\chi$ for these diborides. In addition, there is a conspicuous discrepancy between the calculated contributions to the magnetic susceptibility $\chi_{\rm sum} = \bar{\chi}_{\rm spin} + \bar{\chi}_{\rm orb} + \chi_{\rm dia}$ in Table 2 and the experimental values, $\chi_{\rm exp} = \bar{\chi}$ (Table 1), which can be attributed to the Landau diamagnetic contribution $\chi_{\rm L}$ in Eq. (5). For the diborides of group 4 metals we can evaluate $\chi_{\rm L} \simeq \chi_{\rm exp} - \chi_{\rm sum}$ to be about -10^{-4} cm^3/mol. The relatively large magnitude of this estimate, which far exceeds the free-electron Landau value $\chi_{\rm L}^0$, requires further examination.

It has been established, that small groups of quasi-degenerate electronic states with light effective masses, situated in the close vicinity of the Fermi level $E_{\rm F}$ (about 0.1 eV or closer), yield pronounced and anisotropic orbital diamagnetic contributions to susceptibility in non-transition metals Cd and Zn [25], graphite [26], Be [28], Bi–Sb alloys [27] and even in systems with substantial admixture of *d*- and *f*-states at $E_{\rm F}$ ($YbPb_3$, $YbSn_3$ and $La(In,Sn)_3$ alloys [29]). Such $\chi_{\rm L}$ contributions can be many times larger than the free-electron Landau estimation $\chi_{\rm L}^0$ and this anomalous diamagnetism is determined by a delicate interaction between

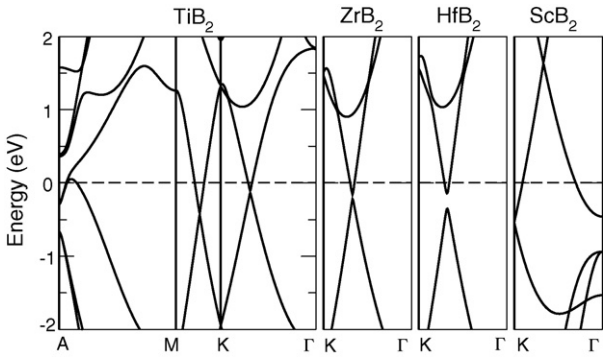

Fig. 5. Energy bands of TiB_2, ZrB_2, HfB_2, and ScB_2along the symmetry directions. The Fermi level is marked by a horizontal dashed line.

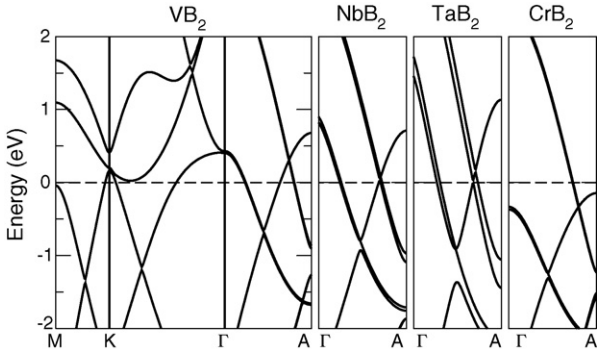

Fig. 6. The energy bands of VB_2, NbB_2, TaB_2, and CrB_2 along the symmetry directions. The Fermi level is marked by a horizontal dashed line.

effective masses, small spin–orbit splittings, and the relative position of E_F. In this connection we should note that the position of E_F with respect to the degeneracy points of $E(k)$ spectrum may be not quite correctly predicted by *ab initio* calculations.

As can be seen in Fig. 5, the present band structure calculations point to the presence of quasi-degenerate hybridized electronic states close to E_F in TiB_2. The bands crossing in the basal plane around the symmetry point K is of particular importance in connection with a manifestation of the anomalously large χ_L, which was found to originate from similar degeneracy points [26–28]. Also, the analogous quasi-degenerate states with small effective masses exist at E_F in the diborides of other group 4 metals, $ZrB_2$and HfB_2, and appear to be slightly affected by the spin–orbital coupling (see directions $K \to \Gamma$ in Fig. 5). On the other hand, as also seen in Fig. 5, for ScB_2, the diboride of the group 3 metal, the corresponding bands crossing lies substantially above E_F. It should be noted, that in the recent de Haas–van Alphen studies [6] the very light cyclotron masses (about 0.1 of the free-electron mass) have been observed in ZrB_2 and HfB_2. This band structure similarity together with the observed close values of $\bar{\chi}$ and $\Delta\chi$ in TiB_2, ZrB_2 and HfB_2 (see Table 1) indicate that the corresponding quasi-degenerate states might determine the diamagnetism of the diborides of group 4 metals.

Available experimental data on susceptibility of the group 5 diborides, (VB_2, NbB_2 and TaB_2, see Table 1), together with the calculated paramagnetic terms χ_{spin} and χ_{orb} from Table 2, also imply the presence of a substantial diamagnetic contribution to χ. Even though VB_2appeared to be paramagnetic, the large χ_{spin} and χ_{orb} contributions have to be almost compensated by χ_L. Also the sign of $\Delta\chi_{orb}$ in Table 2 is not consistent with the experimental $\Delta\chi$ for VB_2. This suggests that only the larger anisotropy of χ_L may compete with $\Delta\chi_{orb}$ and outperform it.

The calculated band structure of the group 5 diborides is presented in Fig. 6, where one can see the presence of quasi-degenerate states with small effective masses at E_F, namely the bands crossing in the $\Gamma \to$ Adirection. We note that the $\Gamma \to$ A bands crossing distinctly approaches E_F in the series VB_2, NbB_2 and TaB_2. One can point out, that for CrB_2 diboride of group 6 the corresponding bands crossing is also not far from E_F. However in this case, as shown below, the spin paramagnetic susceptibility is definitely dominant due to substantial exchange enhancement.

It should be emphasized that rigorous theoretical analysis of χ_L is rather cumbersome procedure, which includes a derivation of accurate multi-band $\mathbf{k}\cdot\mathbf{p}$ models for groups of quasi-degenerate states at E_F, and then exploring a variety of possible options to handle analytical and numerical problems. A choice of scenario for solution can depend on dimension of suitable $\mathbf{k}\cdot\mathbf{p}$ models and a relative position of the Fermi level. This task goes beyond the aims of the present work, and we hope to be able to perform such analysis of χ_L of the diborides in a future. As the first step in this direction, we identified here appropriate electronic states near E_F as possible sources of the large diamagnetism in diborides.

Two other diborides studied in the present work, ScB_2 and CrB_2, appear to be paramagnetic (see Table 1) with expected moderate diamagnetic contributions to χ. As can be seen in Table 2, the field-induced calculated spin susceptibility χ_{spin} is noticeably higher than the spin contribution χ_{ston} calculated within the Stoner model, and the orbital Van Vleck contribution χ_{orb} is comparable to χ_{spin} and necessary to describe the experimental data for ScB_2. Moreover, the calculated anisotropy of χ_{orb} is consistent with the experimentally observed $\Delta\chi$ in ScB_2 and CrB_2.

We note, that for ScB_2 the sum of calculated paramagnetic contributions appears to be lower than the experimental χ. This should be considered as rather expected underestimation for the LSDA *ground state* of ScB_2. Due to the well known overbonding tendency of LSDA [14] the theoretical equilibrium volume is smaller than the experimental one, and this resulted in slightly suppressed values of χ_{spin} and χ_{orb}, which were obtained within the field-induced self-consistent FP-LMTO calculations.

In CrB_2 the Stoner criterion is nearly fulfilled, $IN(E_F) \simeq 1$, with the Fermi level located at the steep slope of $N(E)$ peak where DOS rapidly grows with energy, and the main contribution to $N(E_F)$ comes mostly from *d*-states of Cr (see Fig. 3). The calculated susceptibility enhancement factor S appears to be about 8, which is comparable with earlier estimations ($S \simeq 10$, [3,4]). In the PM phase of $CrB_2$the magnetic susceptibility rises with decreasing temperature and becomes $\chi_{exp} \simeq 6.5 \times 10^{-4}$ cm^3/mol at $T = 90$ K. The extrapolated PM susceptibility, $\chi_{exp}(T \to 0)$, provides the estimation $\chi_{exp}(0) \simeq 7.5 \times 10^{-4}$ cm^3/mol, which is in agreement with the calculated paramagnetic contributions χ_{spin} and χ_{orb} from Table 2.

The band structure calculations for the low temperature AFM helical magnetic structure of $CrB_2$are extremely difficult, and in the present work the electronic structure calculation has been performed for the FM phase of CrB_2, which provided the magnetic moment of 0.8 μ_B, in a fair agreement with the experiment [9,2].

5. Conclusions

The magnetic susceptibility and its anisotropy was studied for the first time on single crystals of the diborides ScB_2, TiB_2, VB_2, ZrB_2, and HfB_2. It was found that the value of anisotropy is strongly dependent on the filling of *p–d* hybridized conduction band, and appeared to be the largest for Ti-group diborides. The *ab initio* electronic structure calculations in an external magnetic field have allowed to evaluate the paramagnetic spin and orbital Van Vleck contributions to magnetic susceptibility of the diborides and their anisotropy. It has been demonstrated that LSDA provides an ade-

quate description of the magnetic properties for ScB_2 and strongly enhanced CrB_2 compounds.

For the diborides of groups 4 and 5, the comparison of the experimental and calculated susceptibilities has revealed a large and anisotropic diamagnetic contribution about -10^{-4} cm^3/mol, which can originate from the generalized Landau diamagnetism of conduction electrons, χ_L. It is anticipated that the large magnitude of χ_L in the diborides of groups 4 and 5 has its origin in the quasi-degenerate electronic states close to the Fermi energy.

Acknowledgments

The authors thank F.A. Sidorenko for giving the single crystalline sample of TiB_2 compound and A. Grechnev for fruitful scientific discussions.

References

[1] T.Y. Kosolapova, Handbook of High Temperature Compounds: Properties, Production, Applications, Hemisphere Pub. Corp, N.Y., 1990.
[2] J. Castaing, P. Costa, V. Matkovich, in: Boron and Refractory Borides, Springer, Berlin, 1977, p. 390.
[3] G.E. Grechnev, N.V. Ushakova, P.D. Kervalishvili, G.G. Kvachantiradze, K.S. Kharebov, Low Temp. Phys. 23 (1997) 217.
[4] P. Vajeeston, P. Ravindran, C. Ravi, R. Asokamani, Phys. Rev. B 63 (2001) 045115.
[5] A.L. Ivanovskii, Phys. Solid State 45 (2003) 1829.
[6] V.B. Pluzhnikov, I.V. Svechkarev, A.V. Dukhnenko, A.V. Levchenko, V.B. Filippov, A. Chopnik, Low Temp. Phys. 33 (2007) 350.
[7] I.R. Shein, A.L. Ivanovskii, J. Phys.: Condens. Matter 20 (2008) 5218.
[8] G. Levchenko, A. Lyashchenko, V. Baumer, A. Evdokimova, V. Filippov, Yu. Paderno, N. Shitsevalova, J. Solid State Chem. 179 (2006) 2949.
[9] S. Funahashi, Y. Hamaguchi, T. Nanaka, E. Bannai, Solid State Commun. 23 (1977) 859.
[10] G. Balakrishnan, S. Majumdar, M.R. Lees, D.M^{c}K. Paul, J. Cryst. Growth 274 (2005) 294.
[11] P. Peshev, J. Etourneau, R. Naslain, Mater. Res. Bull. 5 (1970) 319.
[12] J. Castaing, R. Caudron, G. Toupance, P. Costa, Solid State Commun. 7 (1969) 1453.
[13] S.N. L'vov, M.I. Lesnaya, I.M. Vinitskii, B.A. Kovenskaya, B.G. Makosevskii, Inorg. Mater. 10 (1974) 512.
[14] J.M. Wills, O. Eriksson, M. Alouani, D.L. Price, in: H. Dreysse (Ed.), Electronic Structure and Physical Properties of Solids: The Uses of the LMTO Method, Springer, Berlin, 2000, p. 148.
[15] G.E. Grechnev, R. Ahuja, O. Eriksson, Phys. Rev. B 68 (2003) 64414.
[16] U. von Barth, L. Hedin, J. Phys. C: Solid State Phys. 5 (1972) 1629.
[17] J.P. Perdew, K. Burke, M. Ernzerhof, Phys. Rev. Lett. 77 (1996) 3865.
[18] P.E. Blöchl, O. Jepsen, O.K. Andersen, Phys. Rev. B 49 (1994) 16223.
[19] G.E. Grechnev, A.V. Logosha, I.V. Svechkarev, A.G. Kuchin, Y.A. Kulikov, P.A. Korzhavyi, O. Eriksson, Low Temp. Phys. 32 (2006) 1140.
[20] H. Chung, M.B. Weinberger, J. Yang, S. Tolbert, R.B. Kaner, Appl. Phys. Lett. 92 (2008) 261904.
[21] L. Nordström, O. Eriksson, M.S.S. Brooks, B. Johansson, Phys. Rev. B 41 (1990) 9111.
[22] J. Benkowitsch, H. Winter, J. Phys. F: Met. Phys. 13 (1983) 991.
[23] P. Selwood, Magnetochemistry, Interscience, N.Y., 1956.
[24] J. Banhart, H. Ebert, J. Voitlander, H. Winter, J. Magn. Magn. Mater. 61 (1986) 221.
[25] J.W. McClure, J. Martyniuk, Phys. Rev. Lett. 29 (1972) 1095.
[26] M.P. Sharma, L.G. Johnson, J.W. McClure, Phys. Rev. B 9 (1974) 2467.
[27] G.P. Mikitik, Yu.V. Sharlai, Low Temp. Phys. 26 (2000) 39.
[28] G.E. Grechnev, I.V. Svechkarev, Yu.P. Sereda, Sov. Phys. JETP 75 (1978) 993.
[29] A.E. Baranovskiy, G.E. Grechnev, G.P. Mikitik, I.V. Svechkarev, Low Temp. Phys. 29 (2003) 356.